

Supporting Information to

Volker Strauss^{1*}, Huize Wang¹, Simon Delacroix¹, Marc Ledendecker², Pablo Wessig³

Synthesis	24
Nuclear Magnetic Resonance Spectroscopy of the Raw Products	24
UV-vis and Fluorescence Spectroscopy of the Raw Products.....	25
Nuclear Magnetic Resonance Spectroscopy of the Educts and References	26
Separation of the Raw Products.....	27
Extinction coefficients of CUg	27
Time-correlated Single-Photon Counting of CUg and CUB.....	28
Fluorescence Quantum Yields of CUg	28
Photostability of CUg	29
ESI - mass spectrometry of CUg and CUB.....	29
2D-Correlation NMR of CUg.....	30
DFT calculations of CUg (HPPT).....	31
2D-Correlation NMR of CUB.....	32
Nuclear Magnetic Resonance Spectroscopy of Biuret.....	33
Biuret test with CUB	33
Thermal Mass analysis of CUg and CUB	34
Thermogravimetric Analysis of the Raw Mixture	34
X-ray Photoelectron Spectroscopy of CUB and CUg	35
Nuclear Magnetic Resonance Spectroscopy during Washing of CUp	35
Optical Spectroscopy of dispersions of CUp in H ₂ O.....	36
Nuclear Magnetic Resonance Spectroscopy of a Non-Separated Mixture	36

Synthesis

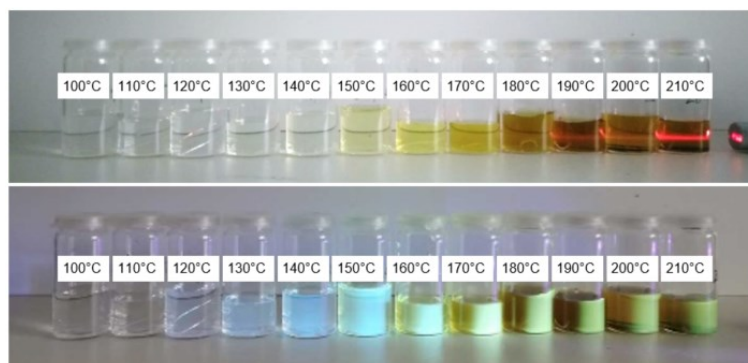


Figure S1. Photograph of aqueous sample solutions of the crude products (conc: 0.2 mg/mL) synthesized at temperatures between 100 – 220°C under illumination with a red laser (top) and under illumination with a UV-lamp (365 nm) (bottom).

Nuclear Magnetic Resonance Spectroscopy of the Raw Products

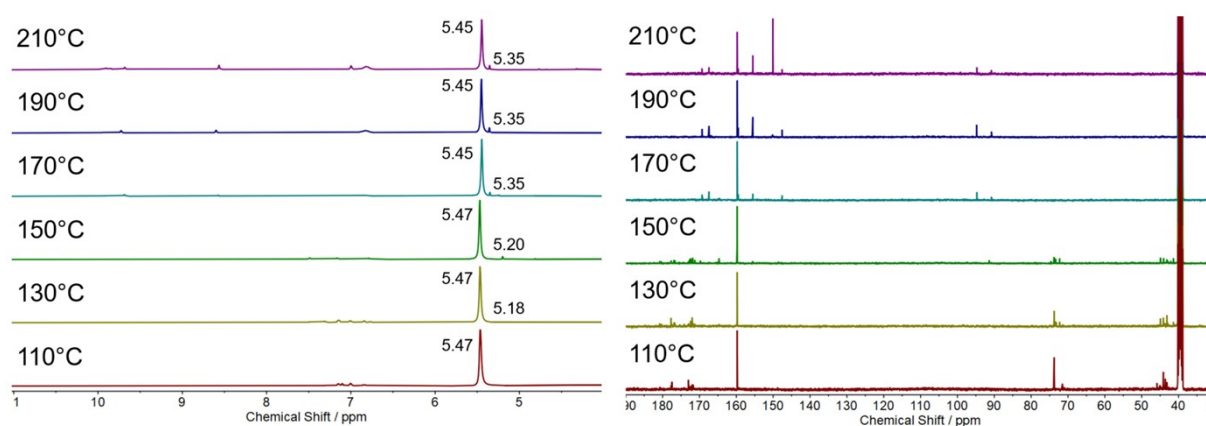


Figure S2. ¹H-NMR (left) and ¹³C-NMR (right) spectra of selected raw products of the CA/U reaction at different temperatures between 110-210°C.

UV-vis and Fluorescence Spectroscopy of the Raw Products

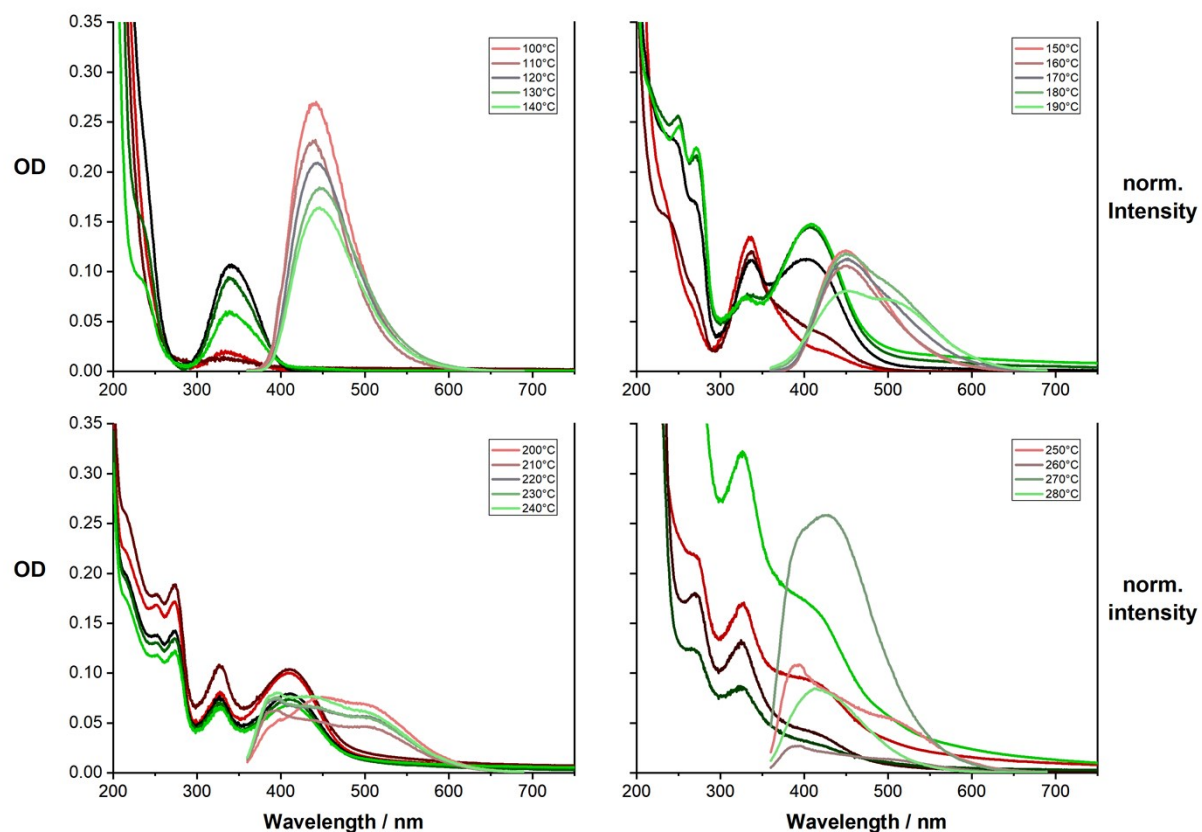


Figure S3. Combined electronic absorption (red to green) and excitation normalized ($\lambda_{\text{ex}} = 350 \text{ nm}$) emission (pale red to pale green) spectra of crude CA/U products (0.013 mg/mL) synthesized at different temperatures between 100 – 290°C; a) 100 – 140°C; b) 150 – 190°C; a) 200 – 240°C; a) 250 – 290°C.

Nuclear Magnetic Resonance Spectroscopy of the Educts and References

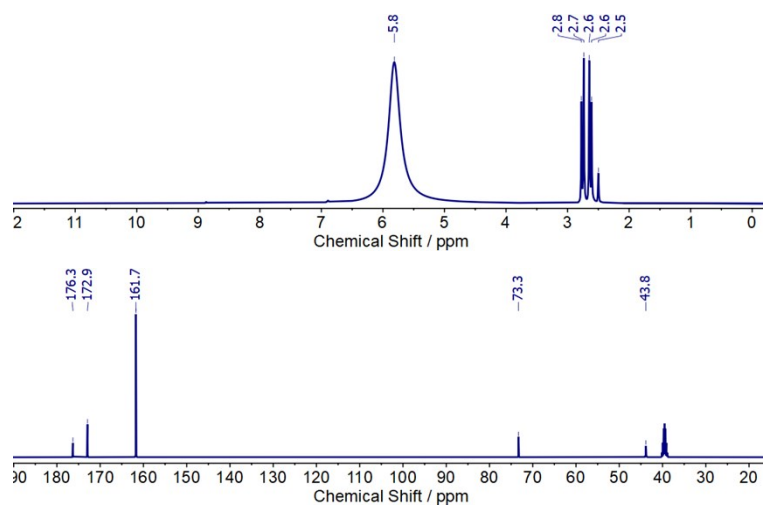


Figure S4. Top: ¹H-NMR (top) and ¹³C-NMR (bottom) spectra of *citric acid* and *urea* in DMSO-d₆.

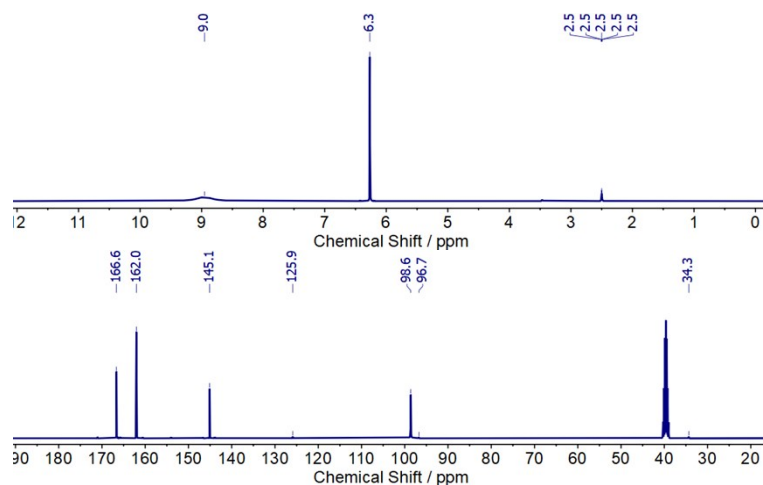


Figure S5. Top: ¹H-NMR (top) and ¹³C-NMR (bottom) spectra of *citrazinic acid* (commercial) in DMSO-d₆.

Separation of the Raw Products

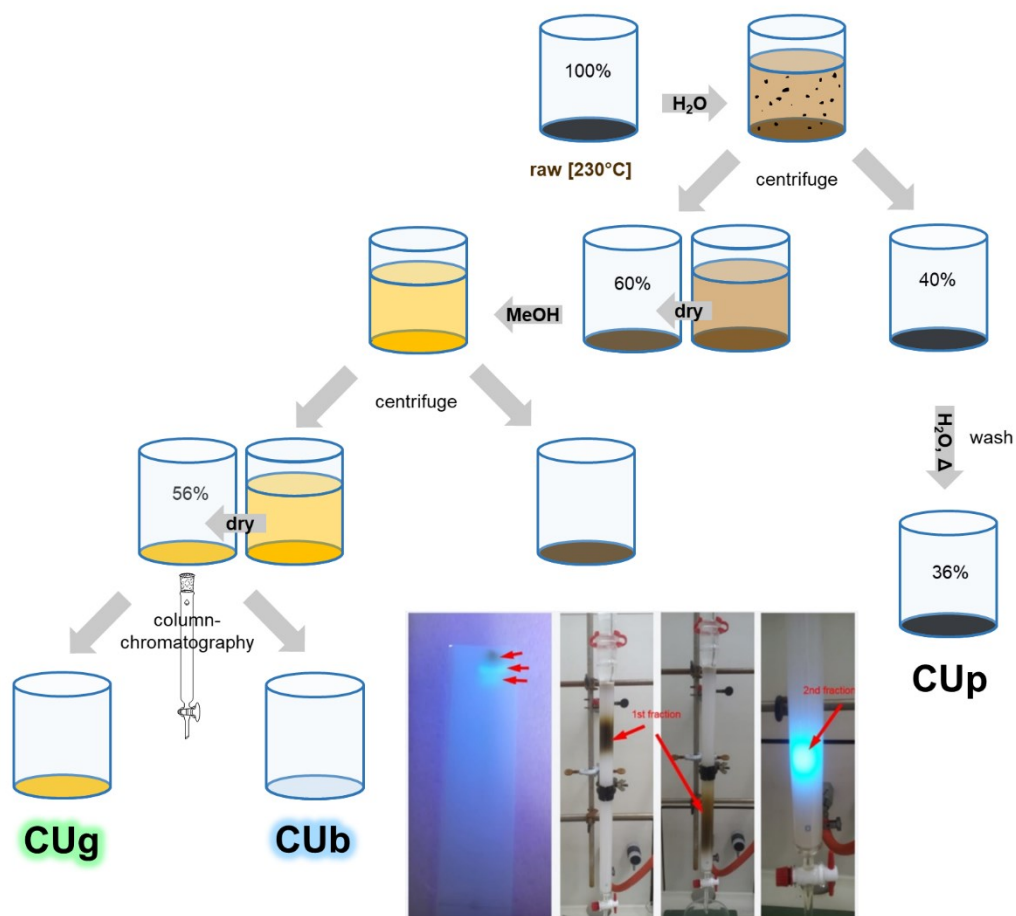


Figure S6. Illustration of the separation process of the raw products obtained from a thermal CA/U reaction.

Extinction coefficients of CUg

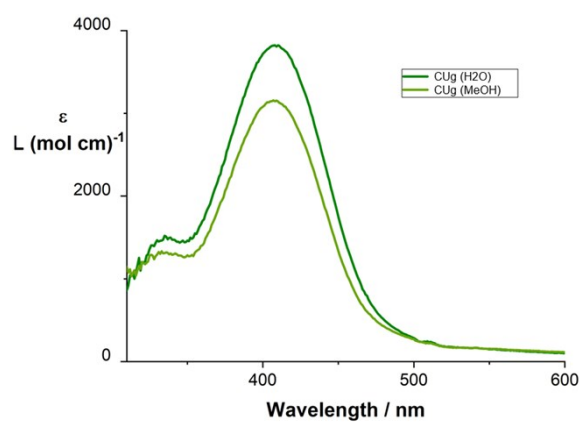


Figure S7. Molar extinction coefficients of CUg in H₂O and MeOH.

Time-correlated Single-Photon Counting of CUb and CUg

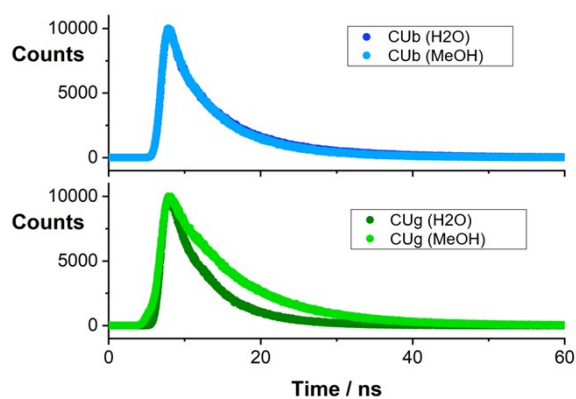


Figure S8. Fluorescence lifetime decay profiles obtained by TCSPC of CUb and CUg in H₂O and MeOH at room temperature obtained upon excitation at 370 or 450 nm, respectively .

Table S1. Fluorescence lifetimes of CUb and CUg in MeOH and H₂O.

		τ_1	A_1	τ_2	A_2
		ns	%	ns	%
CUb	MeOH	3.1	28	7.6	72
	H ₂ O	4.1	45	9.5	55
CUg	MeOH	9.0	100		
	H ₂ O	5.3	100		

Fluorescence Quantum Yields of CUg

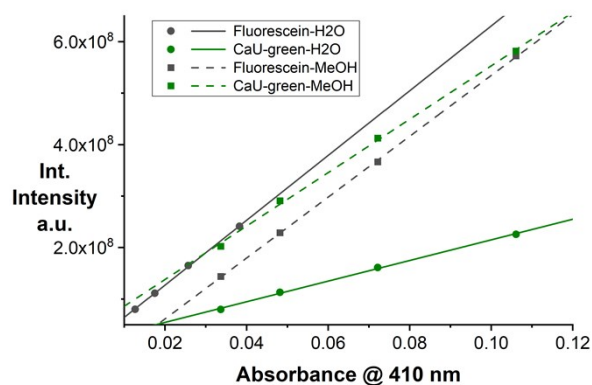


Figure S9. Determination of the fluorescence quantum yields of CUg in H₂O and MeOH using Na-fluorescein as a standard.

Table S2. Fluorescence quantum yields of **CUg** determined by the gradient method using Na-fluorescein as a standard and in MeOH and H₂O.

	solvent	slope	Φ_{Fl} (%)
Na-Fluorescein	H ₂ O	6.30E+09	85 ⁶⁴
	MeOH	5.90E+09	79
CUg	H ₂ O	2.00E+09	27
	MeOH	5.20E+09	70

Photostability of CUg

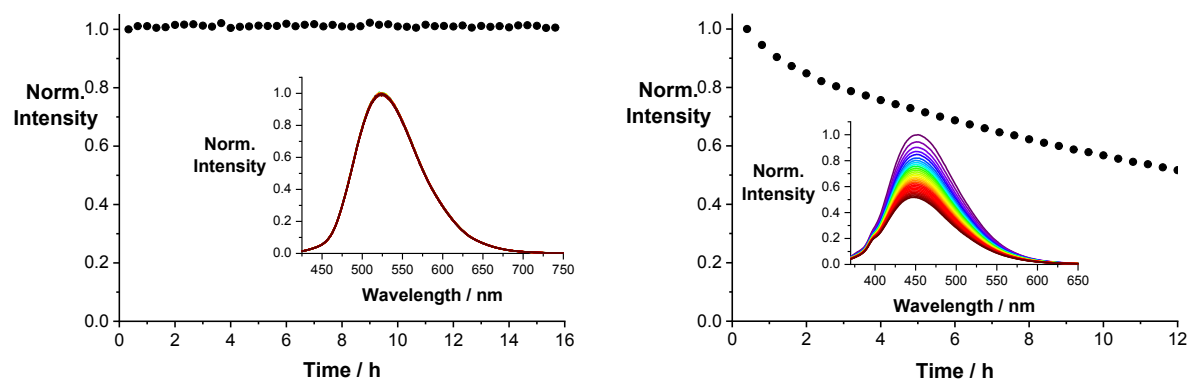


Figure S10. Left: photo-stability measurement of a 8.3×10^{-5} M solution of **CUg** in H₂O. The sample was constantly illuminated for 16h. The inset shows the fluorescence spectra in time intervals of 20 min; Right: Photo-stability measurement of **CUb** in H₂O. The inset shows the fluorescence spectra in time intervals of 24 min from purple to red.

ESI - mass spectrometry of CUg and CUb

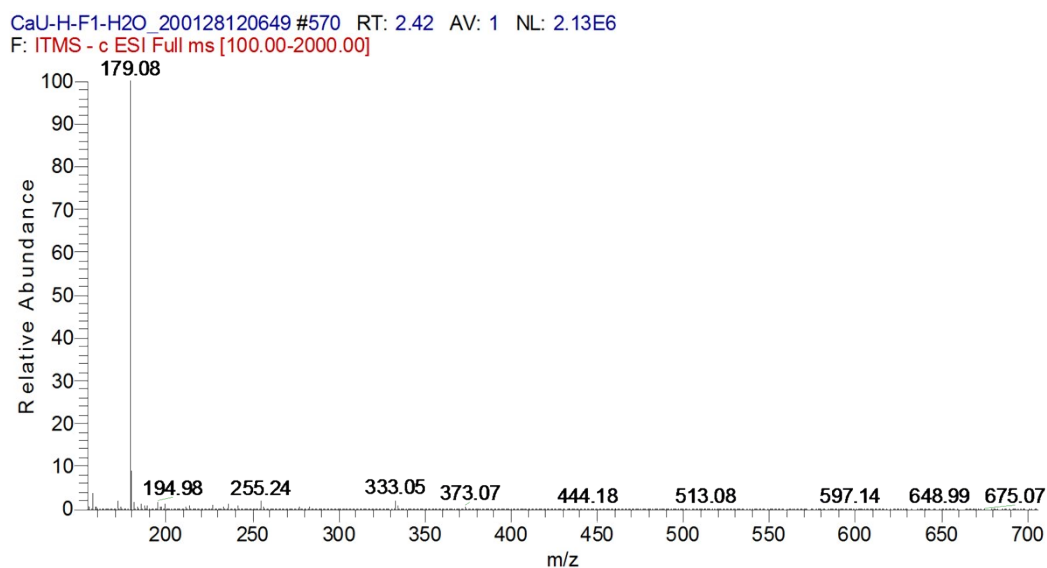


Figure S11. Liquid chromatography-electrospray ionization - mass spectrum of **CUg** obtained in negative ion mode.

CaU-H-F2-H2O_200128131350 #513 RT: 2.18 AV: 1 NL: 7.24E5
 F: ITMS + c ESI Full ms [100.00-2000.00]

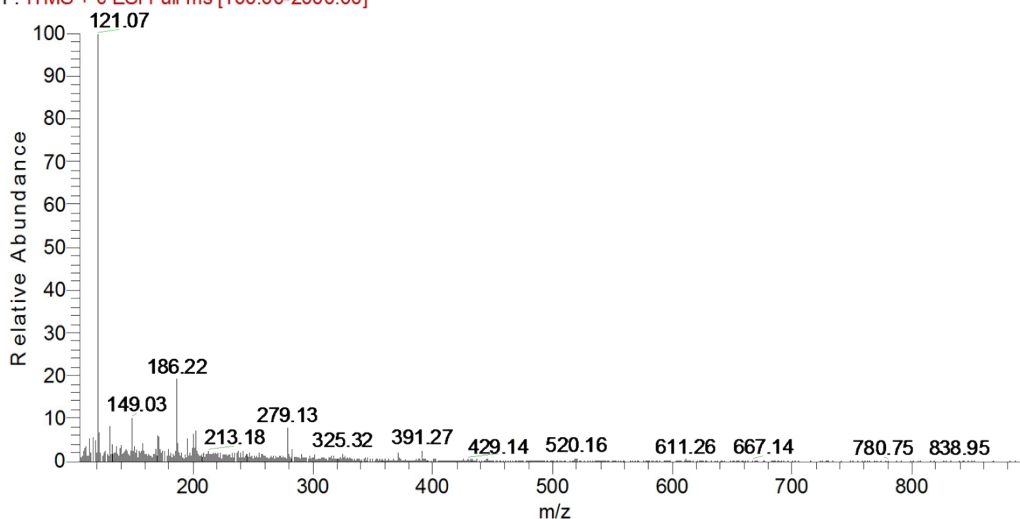


Figure S12. Liquid chromatography – electrospray ionization - mass spectrum of **CUb** obtained in positive ion mode.

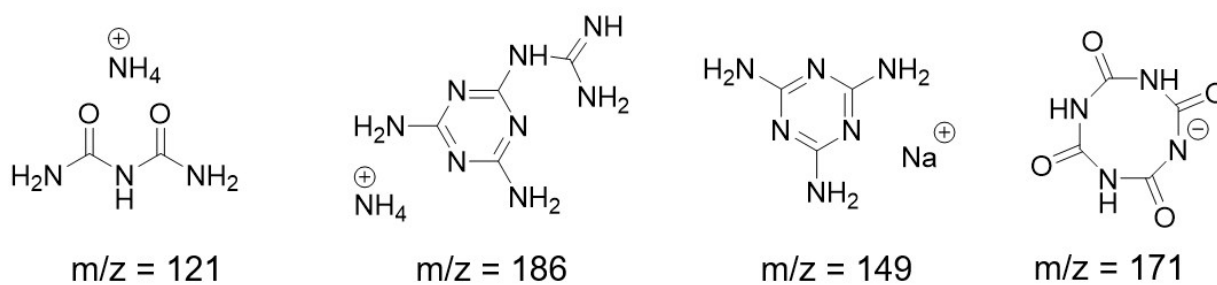


Figure S13. Potential compounds detected in the ESI-mass spectra of **CUb**.

2D-Correlation NMR of **CUg**

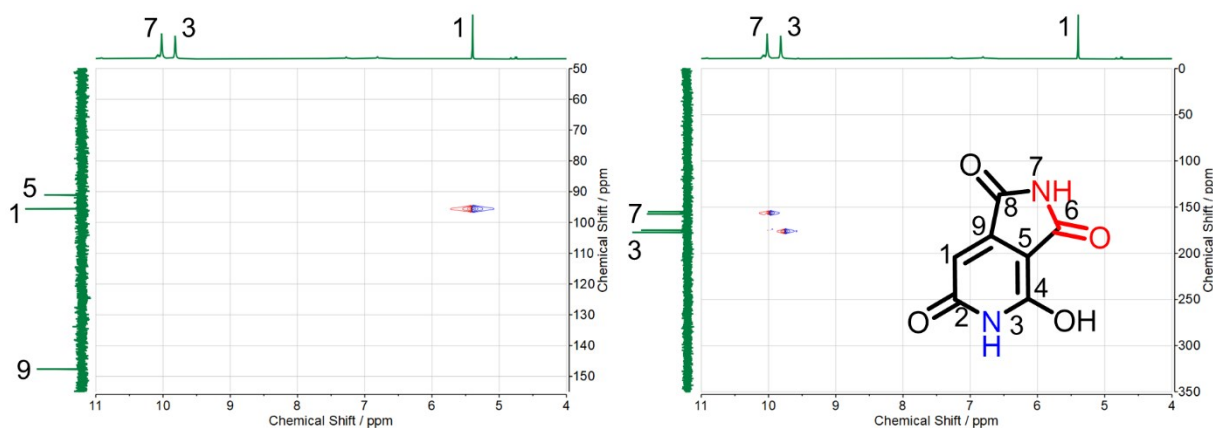


Figure S14. HSQC-C (left) and HSQC-N (right) of **CUg** in DMSO- d_6 showing the direct coupling of ^1H to ^{13}C or ^{15}N , respectively.

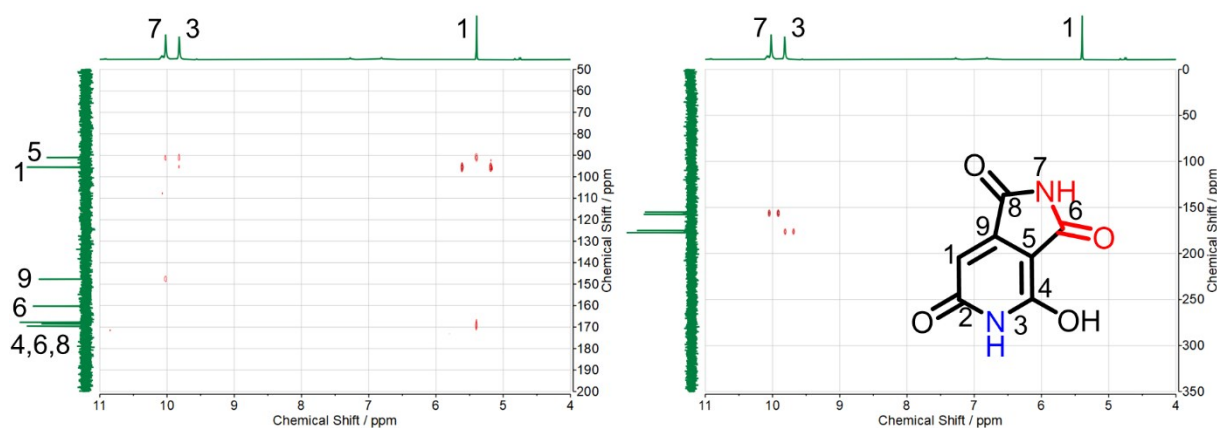


Figure S15. HMBC-C (left) and HMBC-N (right) **CUg** enriched with ^{15}N in DMSO-d_6 showing the three-bond coupling of ^1H to ^{13}C or ^{15}N , respectively.

DFT calculations of CUg (HPPT)

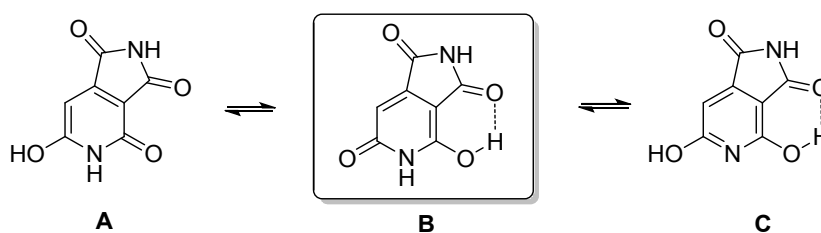
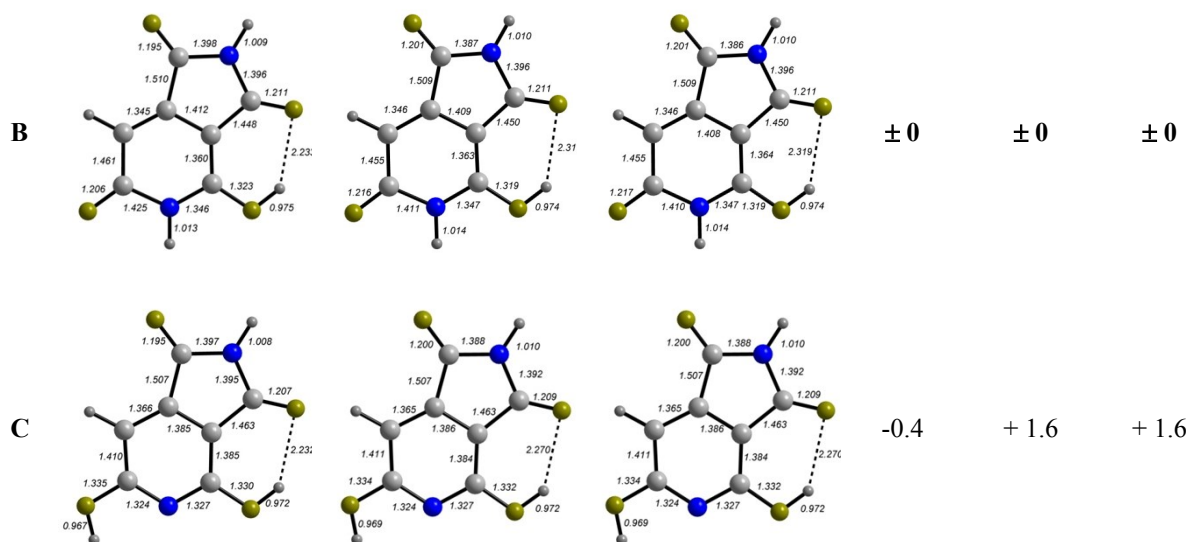


Figure S16. Molecular structures of the tautomeric forms of HPPT.

Table S3. DFT calculated tautomeric forms of HPPT with relative energy values in arbitrary units using M06-2X-D3/def2-TZVP, SCRF: PCM.

Geometry (vacuum)	Geometry (MeOH)	Geometry (H_2O)	E_{REL} (vac.)	E_{REL} (MeOH)	E_{REL} (H_2O)
			+10.9	+ 4.4	+ 4.2



2D-Correlation NMR of CUB

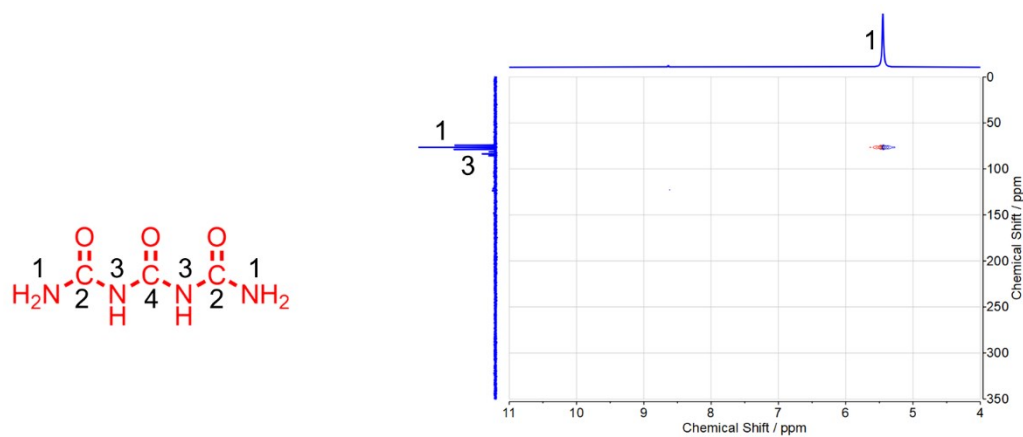


Figure S17. HSQC-N of CUB enriched with ^{15}N in DMSO- d_6 showing the direct coupling of ^1H to ^{13}C or ^{15}N , respectively.

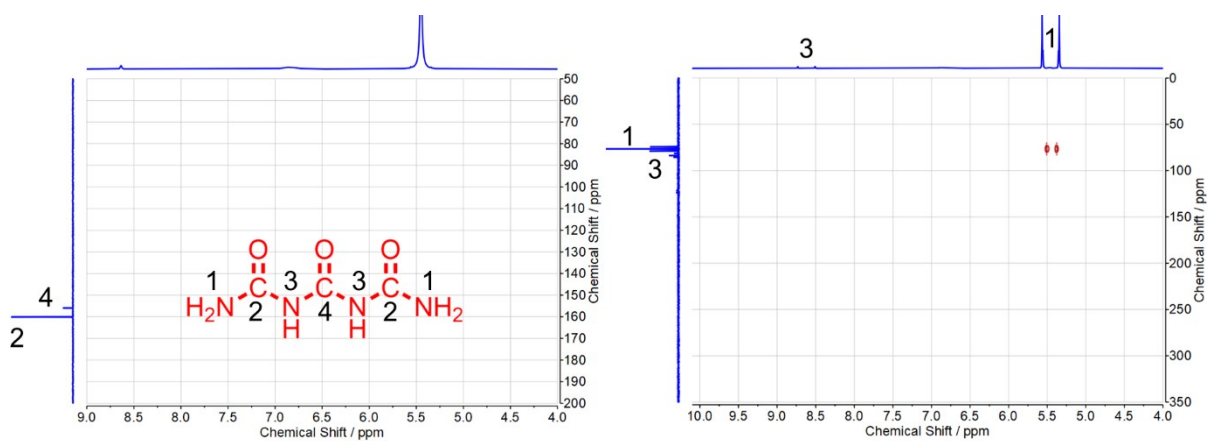


Figure S18. HMBC-C (left) and HMBC-N (right) of **CUB** enriched with ^{15}N in DMSO-d_6 showing the three-bond coupling of ^1H to ^{13}C or ^{15}N , respectively.

Nuclear Magnetic Resonance Spectroscopy of Biuret

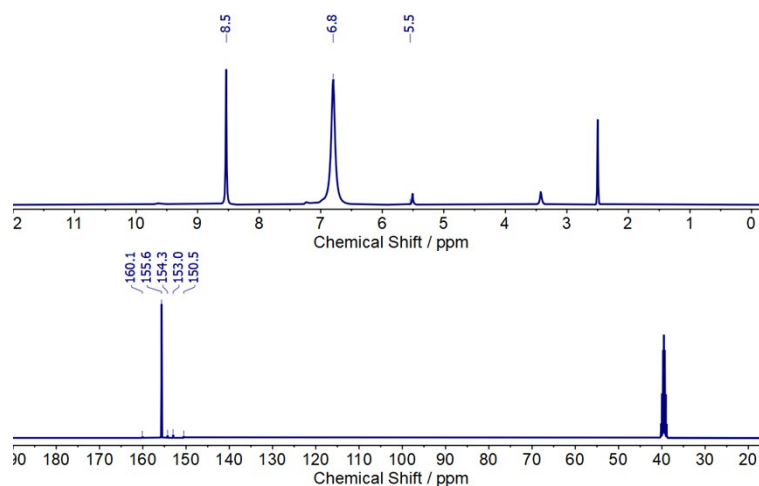


Figure S19. Top: ^1H -NMR (top) and ^{13}C -NMR (bottom) spectra of **biuret** (commercial) in DMSO-d_6 .

Biuret test with **CUB**

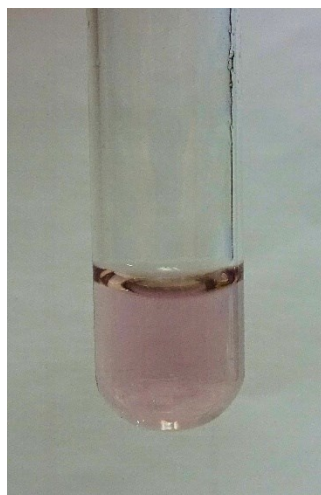


Figure S20. Photograph of a basic solution of **CUB** upon addition of a CuSO_4 solution.

Thermal Mass analysis of CUG and CUB

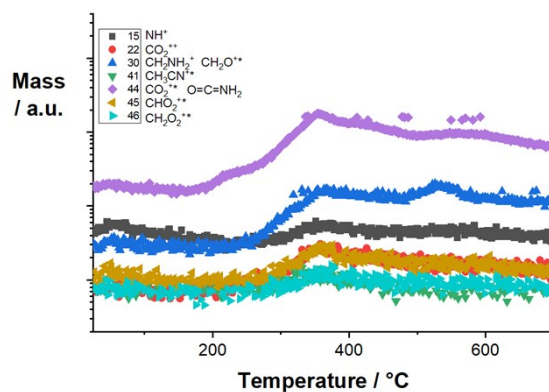


Figure S21. Temperature dependent mass spectrometric analysis of CUG.

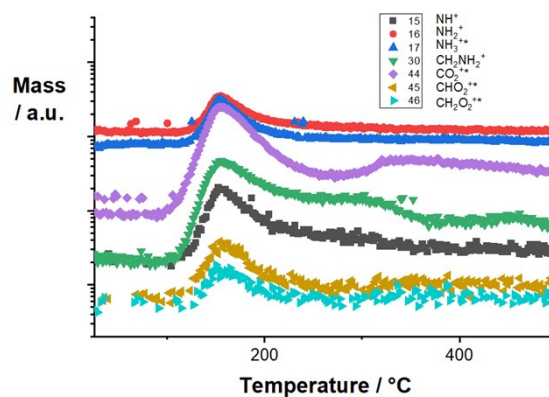


Figure S22. Temperature dependent mass spectrometric analysis of CUB.

Thermogravimetric Analysis of the Raw Mixture

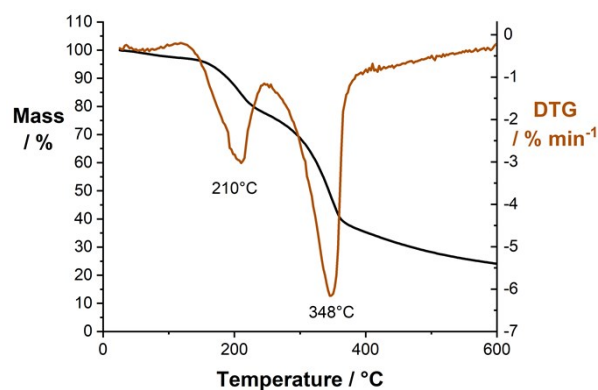


Figure S23. Thermogravimetric analysis of the supernatant of the raw product before column chromatography containing CUG and CUB.

X-ray Photoelectron Spectroscopy of CUB and CUG

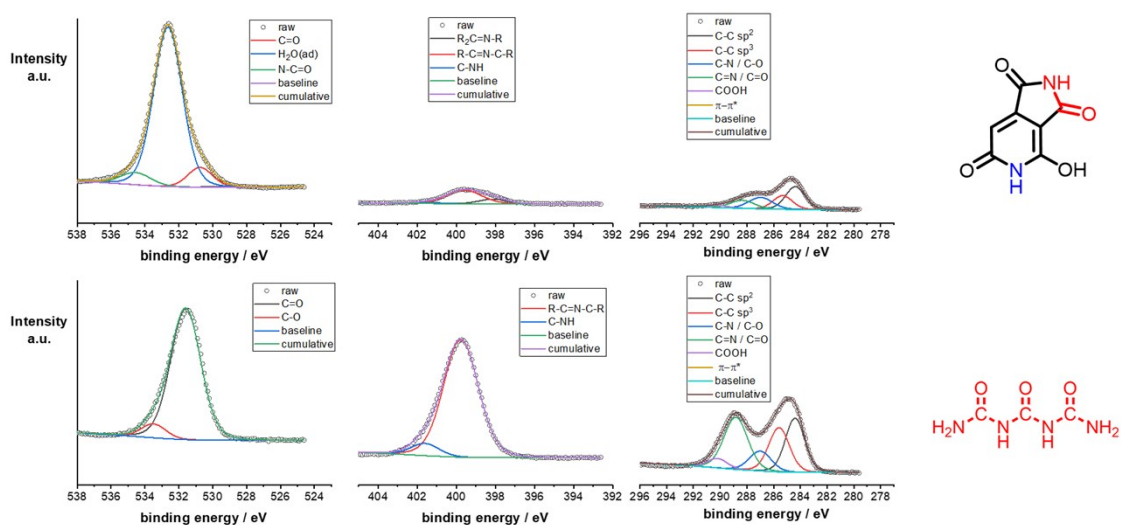


Figure S24. X-ray photoelectron spectra of CUG (top) and CUB (bottom) with emphasis on the C_{1s}, N_{1s}, and O_{1s} regions.

Nuclear Magnetic Resonance Spectroscopy during Washing of CUP

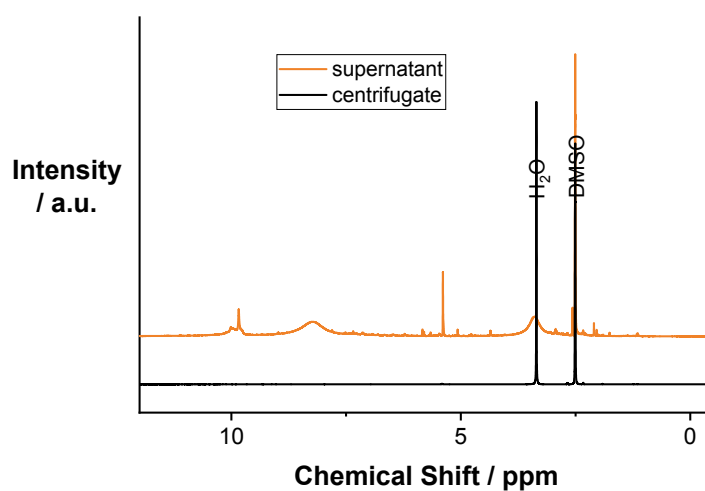


Figure S25. ¹H-NMR spectra of the supernatant and the redispersed centrifugate after washing CUP in H₂O at 95°C in DMSO-d₆.

Optical Spectroscopy of dispersions of CUp in H₂O.

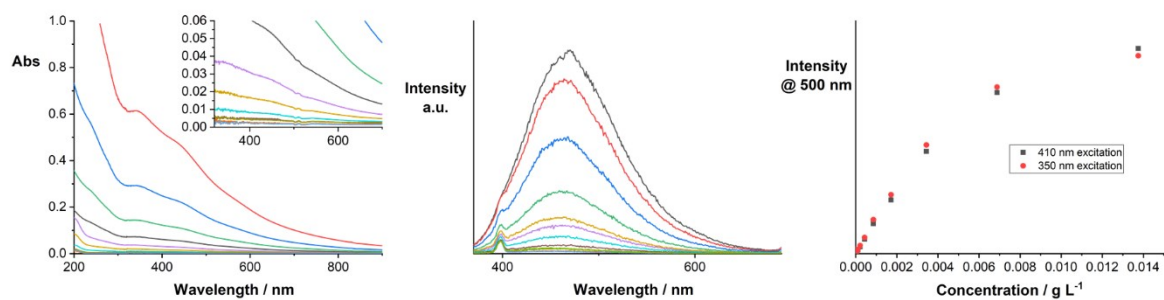


Figure S26. Absorption (left) and fluorescence (center) spectra of CUp in H₂O at room temperature at different concentrations. Right: Fluorescence intensity versus concentration of CUp in H₂O.

Nuclear Magnetic Resonance Spectroscopy of a Non-Separated Mixture

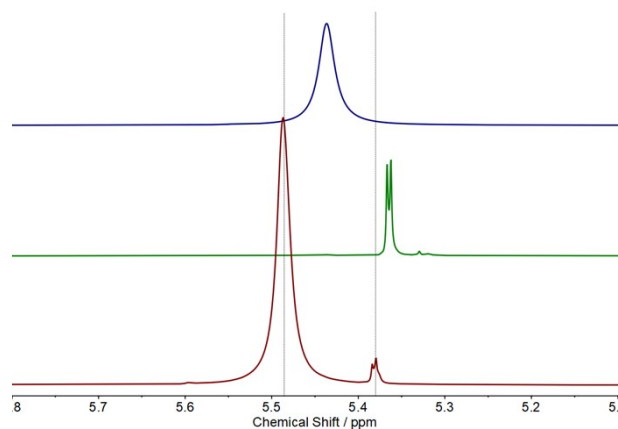


Figure S27. ¹H-NMR spectra of CUb (top), CUg (center) and the non-separated mixture of CUb and CUg (bottom) in DMSO-*d*₆.

References (continued from paper)

64. X.-F. Zhang, J. Zhang and L. Liu, Fluorescence Properties of Twenty Fluorescein Derivatives: Lifetime, Quantum Yield, Absorption and Emission Spectra, *J. Fluoresc.*, 2014, **24** (3), 819–826, 10.1007/s10895-014-1356-5